Equilibrium, kinetic and thermodynamic studies on the adsorption of phenol onto graphene

Yanhui Li [a,*], Qiuju Du [a], Tonghao Liu [a], Jiankun Sun [a], Yuqin Jiao [a], Yanzhi Xia [a], Linhua Xia [a], Zonghua Wang [a], Wei Zhang [b], Kunlin Wang [b], Hongwei Zhu [b], Dehai Wu [b]

[a] Laboratory of Fiber Materials and Modern Textile, The Growing Base for State Key Laboratory, College of Electromechanical Engineering, Qingdao University, 308 Ningxia Road, Qingdao 266071, China
[b] Key Laboratory for Advanced Manufacturing by Material Processing Technology, Department of Mechanical Engineering, Tsinghua University, Beijing 100084, China

ARTICLE INFO

Article history:
Received 25 October 2011
Received in revised form 6 April 2012
Accepted 17 April 2012
Available online 25 April 2012

Keywords:
A. Nanostructures
B. Chemical synthesis
C. Electron microscopy

ABSTRACT

Graphene, a new member of carbon family, has been prepared, characterized and used as adsorbent to remove phenol from aqueous solution. The effect parameters including pH, dosage, contact time, and temperature on the adsorption properties of phenol onto graphene were investigated. The results showed that the maximum adsorption capacity can reach 28.26 mg/g at the conditions of initial phenol concentration of 50 mg/L, pH 6.3 and 285 K. Adsorption data were well described by both Freundlich and Langmuir models. The kinetic study illustrated that the adsorption of phenol onto graphene fit the pseudo second-order model. The thermodynamic parameters indicated that the adsorption of phenol onto graphene was endothermic and spontaneous.

1. Introduction

Phenol and its derivatives are present in the effluents of such industries as petroleum refining, leather and textile manufacturing, steel foundry, olive oil manufacturing and phenol production [1]. Phenols are considered as priority pollutants since they are harmful to aquatic organisms and human beings even at low concentrations. Long-term ingestion of water containing phenols in the human body causes protein degeneration, tissue erosion and paralysis of the central nervous system and also damages the kidney, liver and pancreas [2]. Therefore, it is necessary to remove phenols from industrial wastewaters before being discharged into the aquatic environment.

Many techniques have been employed for removing phenols from aqueous solutions including photocatalytic degradation [3], membrane filtration [4], biological degradation [5], electrochemical oxidation [6], solvent extraction [7]. Out of all these treatment methods, adsorption has been considered as one of the most-widely used and simple treatment approaches for the removal of phenol due to its low cost and high efficiency. Various adsorbents such as chitosan [8], clay [9], activated alumina [10], sludge [11], and activated carbon [1,12] have been screened and used to remove phenol from aqueous solutions. Among them, carbonaceous materials show excellent adsorption capabilities due to their large specific surface area, abundant pore size distribution and controllable surface functional groups. Therefore, the appearance of new type of carbonaceous material always attracts the researchers' attention in using them as adsorbents. For example, fullerene and carbon nanotubes have been quickly used as adsorbents to remove organics [13] and heavy metals [14,15] since their discovery. Their high adsorption capacities and fast adsorption rate make them promising candidates used in environmental protection.

Very recently, a new member of carbon family, graphene, has become a research hotspot due to its unusual physical and mechanical properties such as high carrier concentration and mobility [16], high thermal conductivity [17], and high mechanical strength [18]. These properties hold a great promise for applications in fields like nanoelectronics [19], sensors [20], transistors [21], solar cell [22], ultracapacitors [23], and conducting polymer composites [24]. Preliminary studies showed that graphene has excellent adsorption capabilities for heavy metals such as Pb^{2+}, Cd^{2+}, and Cu^{2+} [25–27] and organics such as methylene blue [28], naphthalene [29] and 1-naphthol [30]. However, up to now no investigations have been carried on using graphene as adsorbent to remove phenol from aqueous solutions.

The objective of this study was to investigate the potential application of graphene as a new adsorbent for the adsorption of phenol from aqueous solutions. The physico-chemical properties of graphene were characterized by transmission electron microscopy (TEM), Fourier transform infrared spectroscopy (FTIR), and Brunauer–Emmett–Teller (BET) analysis. The phenol adsorption

* Corresponding author. Fax: +86 532 85951842.
E-mail addresses: liyanhui@tsinghua.org.cn (Y. Li), xiayzh@qdu.edu.cn (Y. Xia).

properties of graphene were studied through investigating experimental parameters such as pH, dosage, contact time, and temperature. Adsorption isotherm, kinetic and thermodynamic parameters have been estimated from experimental results.

2. Experimental

2.1. Materials

Expandable graphite was purchased from Henglide Graphite Co., Ltd, China. Concentrated sulfuric acid, hydrogen peroxide, potassium permanganate, sodium nitrate, nitric acid, hydrazine hydrate, phenol and sodium hydroxide were purchased from Sinopharm Chemical Reagent Co. Ltd, China.

Graphene was prepared by chemical exfoliation method, which can realize large-scale production of graphene [31]. Graphene oxide was first prepared using a modified Hummers' method [32]. In brief, expandable graphite (5 g) was dispersed into a mixture of concentrated sulfuric acid (230 mL), sodium nitrate (5 g) and potassium permanganate (30 g) at 0 °C. After the mixture was stored in refrigerator at 0 °C for 24 h, it was stirred at 35 °C for 30 min and diluted with deionized water to 690 mL. Then, the mixture was rapidly heated to 98 °C and kept for 30 min, and then diluted with deionized water to 1400 mL. As 30% hydrogen peroxide was added into the mixture, the solutions changed into yellow. The mixture was washed by rinsing with 5% HCl several times. After filtration and drying at 50 °C, the graphene oxide was obtained. 3 g graphene oxide was dispersed into 1500 mL deionized water, then, the mixture was reduced into graphene by adding 200 mL hydrazine hydrate solution (50%). As the solution pH reached 6.5 after rinsing, graphene was filtrated, dried, and stored for further use.

2.2. Adsorbent characterization

Morphology and structure of graphene were characterized by TEM (JEM-2100F). Bulk dry weight-based C, H, and N contents of graphene were determined using an elemental analyzer (Elementar, Germany) with the oxygen content calculated by mass difference. The Brunauer–Emmett–Teller (BET) surface area, pore volume, and pore diameter of graphene were determined from the N_2 adsorption–desorption at −196 °C using a Micrometric ASAP 2000 system. Functional groups of graphene were analyzed by a Perkin-Elmer-283B FTIR spectrometer within the wave number range 400–4000 cm^{-1}. Zeta potentials of graphene, which were dispersed in deionized water by sonication for 20 min before measurement, were measured with a Malvern zetameter (Zetasizer 2000, UK). The isoelectric point (IEP) of graphene was determined by plotting zeta potentials versus solution pH.

2.3. Batch adsorption experiments

Phenol stock solution (100 mg/L) was prepared by dissolving phenol in deionized water and further diluted to the required concentrations before used. The isotherms were determined by a batch equilibration technique at 285 K (room temperature), 313 K, and 333 K. Graphene (0.05 g) and phenol solution (100 mL) with initial concentrations of 10–60 mg/L were added to a 150 mL conical flask for adsorption experiments. The initial pH of adsorbent suspension was 6.3, so it was maintained at 6.3 by dropwise addition of 0.1 M HNO_3 or 0.1 M NaOH during the adsorption processes at every 12 h intervals. The flasks were sealed with glass stoppers and shaken at 100 rpm in a shaker (HZQ-F160) for 48 h. After centrifugation at 7500 rpm for 5 min, final phenol concentrations of supernatants were determined by measuring the absorbance of the samples at the absorbance maximum wavelength of 270 nm by a UV–visible spectrophotometer (TU-1810, Beijing Purkinje Co., Ltd). The uptake of the adsorbate at equilibrium, q_e (mg/g), was calculated by:

$$q_e = \left(\frac{C_0 - C_e}{m}\right)V \quad (1)$$

where C_0 and C_e were initial and equilibrium concentrations of phenol (mg/L), respectively, m was the mass of adsorbent (g) and V was volume of the solution (L).

The effect of pH on phenol adsorbed by graphene was studied in a pH range of 2.3–11.5 and 285 K. The pH of 100 mL solution with phenol concentration 60 mg/L was adjusted using 0.1 M HNO_3 or 0.1 M NaOH. The samples were separated and analyzed after 48 h. In dosage studies, different amounts (0.05–0.17 g) of adsorbents were added into 100 mL solution with phenol concentration of 50 mg/L and shaken at pH 6.3 and 285 K.

The procedures of kinetic experiments were basically identical to those of equilibrium tests. The aqueous samples were taken at preset time intervals and the concentrations of phenol were measured.

3. Results and discussion

3.1. Characterizations of graphene

TEM image (Fig. 1) shows that graphene film is transparent, which is usually rippled and entangled due to partial overlapping of graphene sheets, Atomic force microscopic image shows that graphene sheets have single or two layers [33]. The elemental analysis depicts the composition of graphene as C, 91.46%; N, 4.35%; H, 0.04%; O, 4.15%. The nitrogen adsorption/desorption isotherm of graphene and the pore size distribution based on BJH method were presented in Fig. 2. According to the IUPAC classification, graphene isotherm exhibits type IV with a hysteresis loop. A rapid increase in the volume of adsorbed N_2 is observed in the P/P_0 range of 0.45–0.90. This obvious increase may be attributed to the capillary condensation, indicating the good homogeneity of graphene and fairly small pore size. The apparent step in the adsorption branch combined with the sharp decline in the desorption branch is an obvious indication of mesoporous structure characteristic of graphene [34]. The pore size distribution (Fig. 2, insert) calculated from the desorption branch of the isotherm shows a monomodal distribution in the mesopore region (2–10 nm) due to the single hysteresis loop, indicating the exquisite quality of graphene. The BET surface area, pore volume, and pore diameter of graphene are 305.78 m^2/g, 0.33 cm^3/g, and 3.63 nm, respectively.

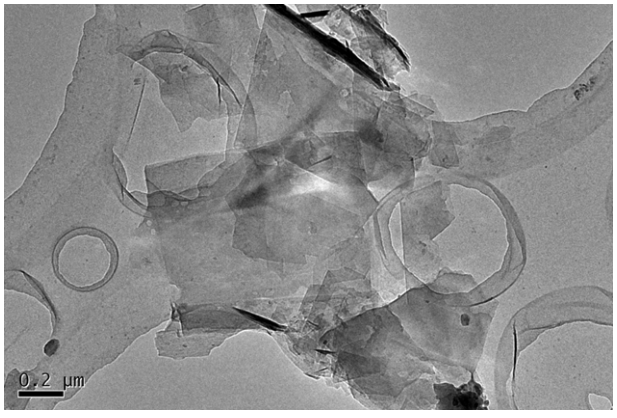

Fig. 1. TEM image of graphene.

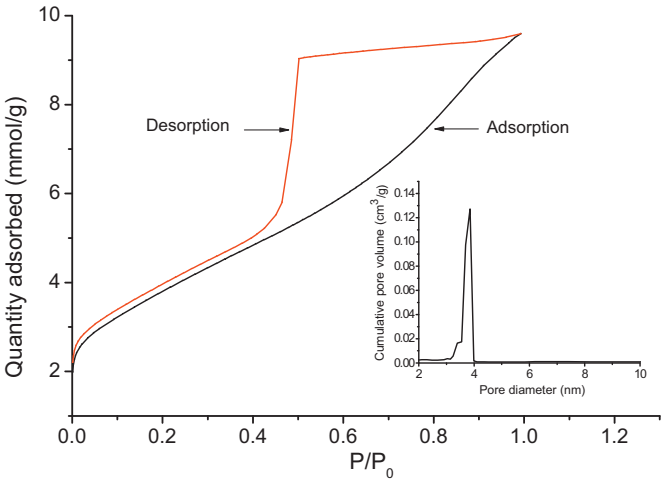

Fig. 2. Nitrogen adsorption–desorption isotherm and pore size distribution (insert) for graphene.

The FT-IR spectrum of graphene was shown in Fig. 3. The strong peak at 3420 cm^{-1} can be assigned to stretching vibration of OH groups. The bands at 2920 cm^{-1} and 2360 cm^{-1} are associated with the stretching of CH_2 and CH_3 groups assigned to methylene stretch [35]. The bands at 1630 cm^{-1} and 1410 cm^{-1} are indicative of the existence of asymmetric and symmetric stretching vibration of C=O groups [36], suggesting that the reduction of graphene oxide is incomplete, this result is supported by the existence of O in the sample through element analysis. The band at 1100 cm^{-1} may be attributed to the appearance of C–N groups originated from the incomplete reduction of the graphene oxide.

Zeta potential is a physical parameter to quantify the electrical potential of the solid particle surface. Fig. 4 shows the surface charge distribution of graphene. The isoelectric point (IEP) of graphene is 5.5 determined by the pH location where zeta potential equals zero. This indicates that at pH < 5.5 graphene has positive surface charge and can act as anion exchanger, while at pH > 5.5 the surface charge of graphene is negative, which benefits for adsorbing cations.

3.2. Adsorption studies

3.2.1. Effect of pH

The pH of adsorption medium is one of the most important parameters to determine the adsorption property of an adsorbent due to its effect not only on surface charge of the adsorbent, but also on the degree of ionization and speciation of adsorbate [37]. At

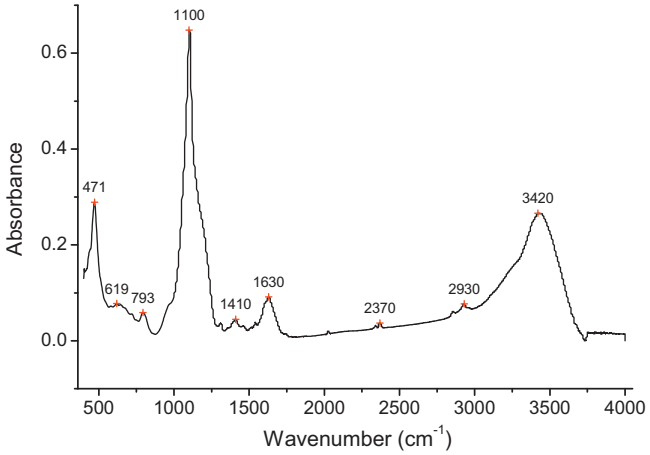

Fig. 3. FTIR spectrum of graphene.

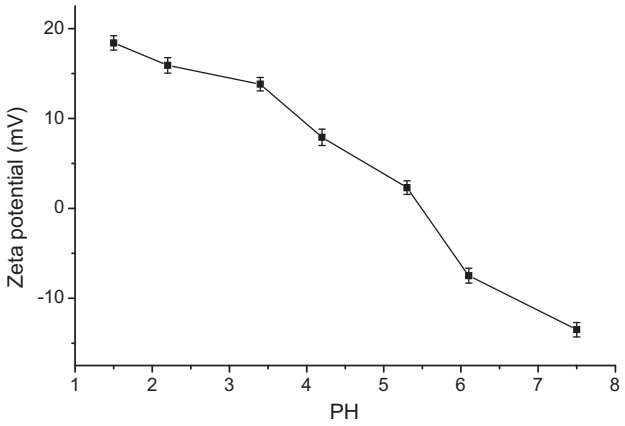

Fig. 4. Zeta potential curve versus pH of graphene. The error bar represents the standard deviations ($n = 3$).

higher pH phenol can dissociate to form phenolate anions. The ionization is dependent on the solution pH and the ionic fraction of phenolate ions, φ_{ions}, can be calculated from the equation [38]:

$$\varphi_{ions} = \frac{1}{[1 + 10^{(pK_a - pH)}]} \quad (2)$$

It is apparent that φ_{ions} increases with the pH value. The pK_a of phenol is 10, so below this pH phenol is considered a neutral molecule and above this value is found as anionic species. Fig. 5a

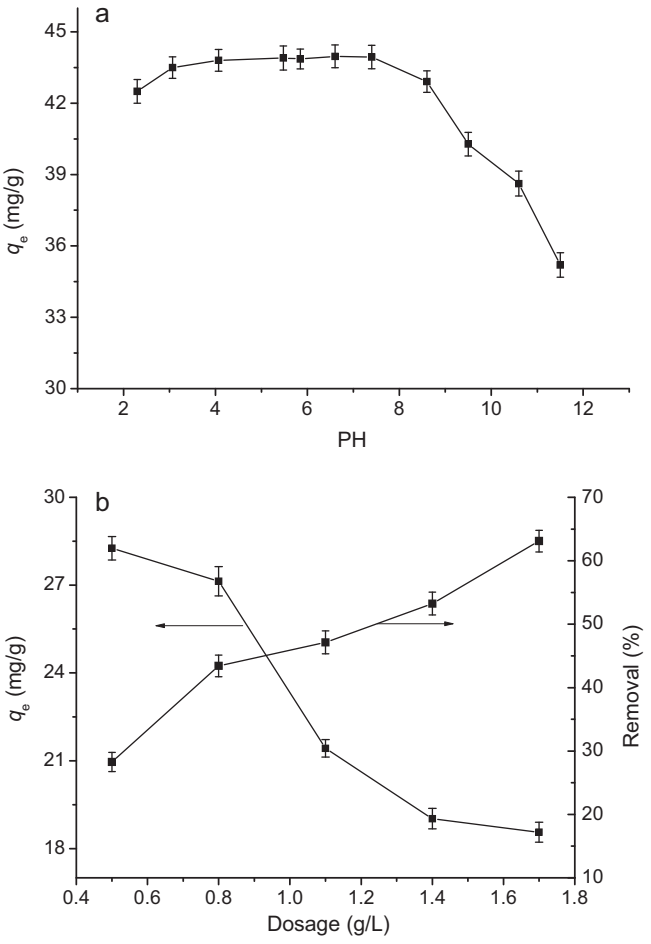

Fig. 5. Effect of (a) pH and (b) dosage on phenol adsorbed by graphene. The error bar represents the standard deviations ($n = 3$).

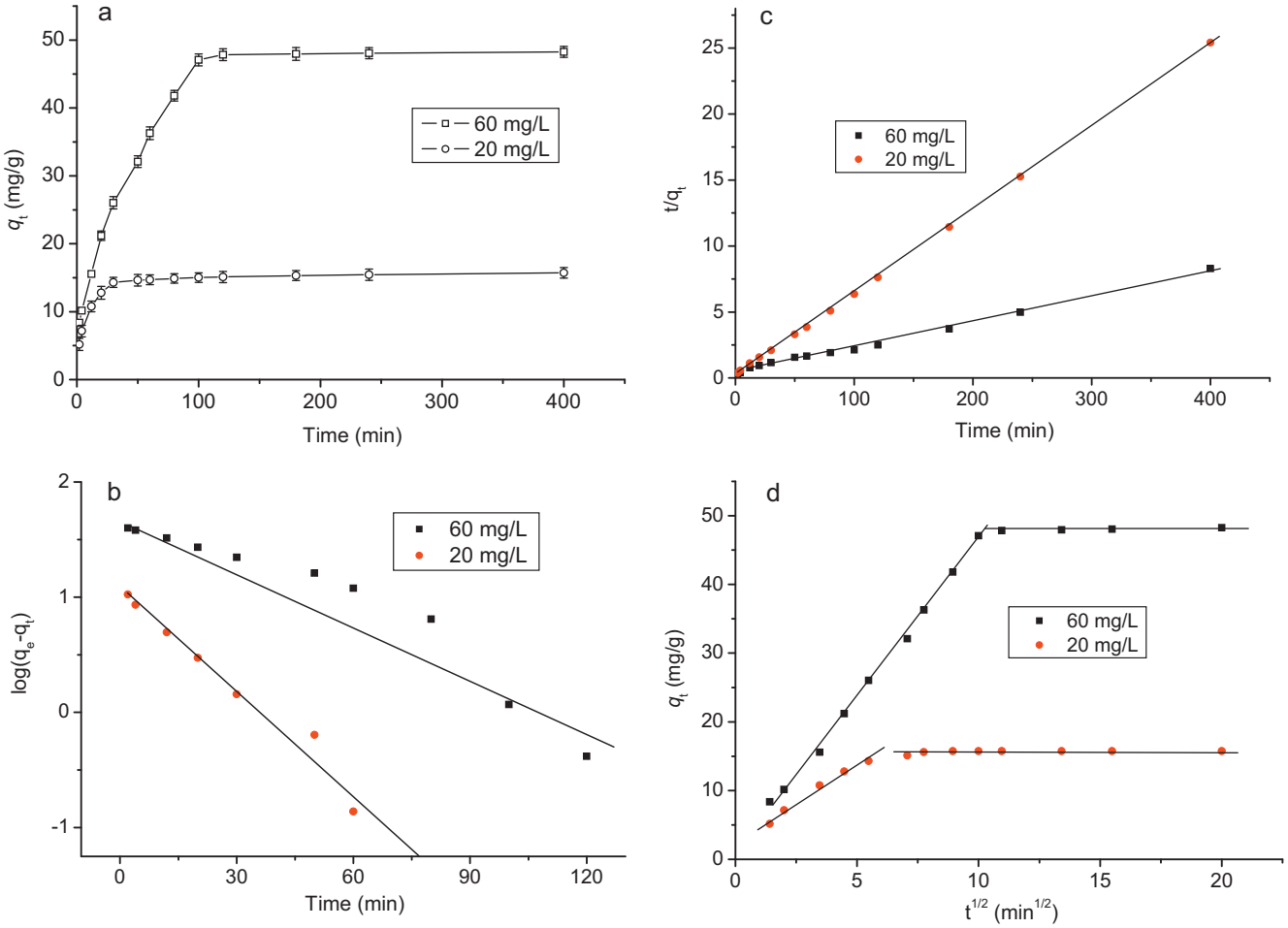

Fig. 6. (a) Time effect on phenol adsorbed by graphene, (b) pseudo-first-order, (c) pseudo-second-order, and (d) intraparticle diffusion models. The error bar represents the standard deviations (n = 3).

shows that at the low pH (<4.0) the adsorption capacity is a little bit low, this is due to that the surface charge of graphene is positive and the H^+ ion concentration in solution is high, therefore competition between H^+ and phenol could occur to reduce the adsorbent–adsorbate interaction. The adsorption capacity at the pH range from 4.0 to 6.6 is high. This may be due to the functional groups formed on the surface of graphene which increase their surface complexation capability [28] and the π–π stacking interaction between phenol molecules and the surface of graphene [30]. As pH > 10, phenol dissociates and forms negatively charged chlorophenolate anions, while the surface charge of graphene is negative, the electrostatic repulsion between the adsorbent and adsorbate lowers the adsorption capacity.

3.2.2. Effect of dosage

The effect of adsorbent dosage on the percentage removal and adsorption capacity of phenol on graphene were shown in Fig. 5b. As the adsorbent dosage increases from 0.5 to 1.7 g/L, the phenol percentage removal increases from 28.3 to 63.1%, whereas the adsorption capacity decreases from 28.3 to 18.6 mg/g. The increased percentage removal of phenol with increasing graphene dose could be due to the increased absolute adsorption surface [39], while the decreased adsorption capacity may be attributed to that the decreased total surface area of the adsorbent, the increased diffusion path length of phenol molecules and the unsaturated adsorption sites caused by the increase in adsorbent dose at constant phenol concentration and volume [39].

3.3. Adsorption kinetics

The effect of contact time on phenol adsorbed by graphene was studied and shown in Fig. 6a. It can be seen that the adsorption amounts of phenol on graphene increases quickly at the initial stage and then increase further but slowly afterward. The initial fast adsorption is due to the special one-atom-thick layered structure of graphene, which makes phenol contact immediately with the active sites on the surface of graphene. With further increasing time, the diminishing availability of the remaining active sites and the decrease in the driving force make it take long time to reach equilibrium.

To analyze the adsorption kinetics of the phenol, pseudo first-order [40] and pseudo second-order models [41] were tested.

The pseudo-first-order model is widely used for adsorption from the liquid phase. Its linearized form can be presented as follows:

$$\log(q_e - q_t) = \log q_e - \frac{k_1}{2.303} t \quad (3)$$

where k_1 is the Lagergren rate constant of adsorption (1/min), q_e (mg/g) and q_t (mg/g) are the quantities of the adsorbed phenol at equilibrium and at time t, respectively.

Plots of $\log(q_e - q_t)$ versus t were shown in Fig. 6b, The values of k_1 and q_e were determined from the slope and intercept of linear fitting (Fig. 6a) and listed in Table 1. The lower coefficients of determination ($R^2 < 0.9738$) suggest that the plots of $\log(q_e - q_t)$

Table 1
Parameters of the pseudo first-order, pseudo second-order and intra-particle diffusion models for phenol adsorbed by graphene.

Kinetic model	Parameters	Values	
		20 (mg/L)	60 (mg/L)
Pseudo-first-order	q_e (mg/g)	11.74	59.35
	k_1 (1/min) $\times 10^{-3}$	2.00	35.93
	R^2	0.9738	0.9200
Pseudo-second-order	q_e (mg/g)	15.95	51.81
	K_2 (g/(mg min)) $\times 10^{-3}$	19.35	0.94
	R^2	0.9998	0.9949
Intraparticle diffusion	k_I	2.25	4.55
	R^2	0.9858	0.9975
	k_{II}	0.09	0.15
	R^2	0.9711	0.9989

against t do not give a straight line, and consequently, this indicates that the adsorption of phenol onto graphene does not fit the pseudo first-order model.

The pseudo-second-order model can be represented by the following linear equation:

$$\frac{t}{q_t} = \frac{1}{k_2 q_e^2} + \frac{t}{q_e} \tag{4}$$

where k_2 is the pseudo second-order rate constant of adsorption (g/(mg min)). The values of q_e and k_2 were determined from the slope and intercept of the plots of t/q_t against t.

The validity of pseudo second-order model was checked by the fitted straight line (Fig. 6c). The corresponding kinetic parameters and the determination coefficients were summarized in Table 1. The high coefficients of determination (R^2) and similarity between the experimental capacities at equilibrium and the calculated capacities from the model indicate that the pseudo second-order model fits the experimental data quite well.

For a solid liquid adsorption process, to analyze the rate controlling steps such as mass transport and chemical reaction processes is very beneficial for elaborating the adsorption mechanism. The adsorption reaction is usually divided into the following steps [42]: (1) transport of solute ions from the boundary film to the external surface of the biosorbent (film diffusion); (2) transfer of ions from the surface to the intraparticular active sites (particle diffusion); (3) adsorption of ions by the active sites of adsorbent. Weber and Morris model is a widely used intraparticle diffusion model to predict the rate controlling step [43]. The rate constants of intraparticle diffusion (k_{id}) at the stage i were determined using the following equation:

$$q_t = k_{id} t^{1/2} + C_i \tag{5}$$

where q_t is the amount adsorbed phenol at time t, $t^{1/2}$ is the square root of the time, C_i is the intercept at stage i. The value of C_i is related to the thickness of the boundary layer. The larger C_i represents the greater effect of the boundary layer on ion diffusion. The plots of q_t versus $t^{1/2}$ at different initial phenol concentrations show multilinearity characterizations (Fig. 6d), indicating that two steps occurred in the adsorption process. The intraparticle diffusion parameters and the determination coefficients were summarized in Table 1. The first sharp section is the external surface adsorption or instantaneous adsorption stage. The second subdued portion is the gradual adsorption stage, where intraparticle diffusion is rate-controlled [44]. The larger slopes of the first sharp sections indicate that the rate of phenol removal is higher in the beginning stage due to the instantaneous availability of large surface area and active adsorption sites. The lower slopes of the second subdued portion are due to that the decreased concentration gradients make phenol molecule diffusion in the micropores of adsorbent take long time, thus leading to a low removal rate. The obvious two steps of the plots as well as their deviation from the origin suggests that the intraparticle diffusion is not the only rate controlling step for the adsorption of phenol onto graphene [45].

Table 2
Parameters of the Freundlich and Langmuir adsorption isotherm models for phenol adsorbed by graphene.

T (K)	Freundlich			Langmuir		
	n	k_F	R^2	q_{max}	k_L	R^2
285	1.64	3.33	0.9927	27.17	0.0388	0.9961
313	1.64	4.77	0.9946	49.51	0.0461	0.9946
333	1.72	6.47	0.9964	53.19	0.0587	0.9921

3.4. Adsorption isotherms

Adsorption isotherms can be generated based on Freundlich and Langmuir models. The Freundlich equation [46] is an empirical equation based on adsorption on a heterogeneous surface. The equation is commonly represented by:

$$\ln q_e = \ln k_F + \frac{1}{n} \ln c_e \tag{6}$$

where k_F and n are the Freundlich constants characteristics of the system, indicating the adsorption capacity and the adsorption intensity, respectively. From the slope and intercept of straight portion of the linear plot obtained by plotting $\ln q_e$ against $\ln C_e$, the values of Freundlich parameters were calculated and listed in Table 2.

The Langmuir model supposes that uptake of metal ions occurs on a homogenous surface by monolayer adsorption without any interaction between adsorbed ions, with homogeneous binding sites, equivalent sorption energies, and no interaction between adsorbed species. Its mathematical form is written as [47]:

$$\frac{C_e}{q_e} = \frac{C_e}{q_{max}} + \frac{1}{q_{max} k_L} \tag{7}$$

where q_{max} is the maximum adsorption capacity corresponding to complete monolayer coverage (mg/g) and k_L is a constant indirectly related to adsorption capacity and energy of adsorption (L/mg), which characterizes the affinity of the adsorbate with the adsorbent. A straight line is obtained when C_e/q_e was plotted against C_e and q_{max} and k_L could be calculated from the slopes and intercepts (Table 2)

As seen from the table, the high correlation coefficients (>0.9921) of both equations are considerably well obtained at all temperatures, indicating that both isotherms fit the experimental adsorption data well. The higher values of k_F indicate that graphene has a higher adsorption capacity and affinity for phenol, especially at 333 K. The n values are greater than unity, indicating that the adsorption is favorably adsorbed by graphene at all temperatures studied. [48].

The values of q_{max} determined from Langmuir equation increases from 27.17 to 53.19 mg/g as temperature increases from 285 to 333 K, it is higher than that of multiwalled carbon nanotubes (14.41 mg/g) [49], suggesting that graphene is a promising adsorbent to remove phenol from aqueous solutions.

3.5. Adsorption thermodynamic study

Temperature effect on adsorption of phenol on graphene was carried out at three different temperatures, i.e., 285, 313 and 333 K

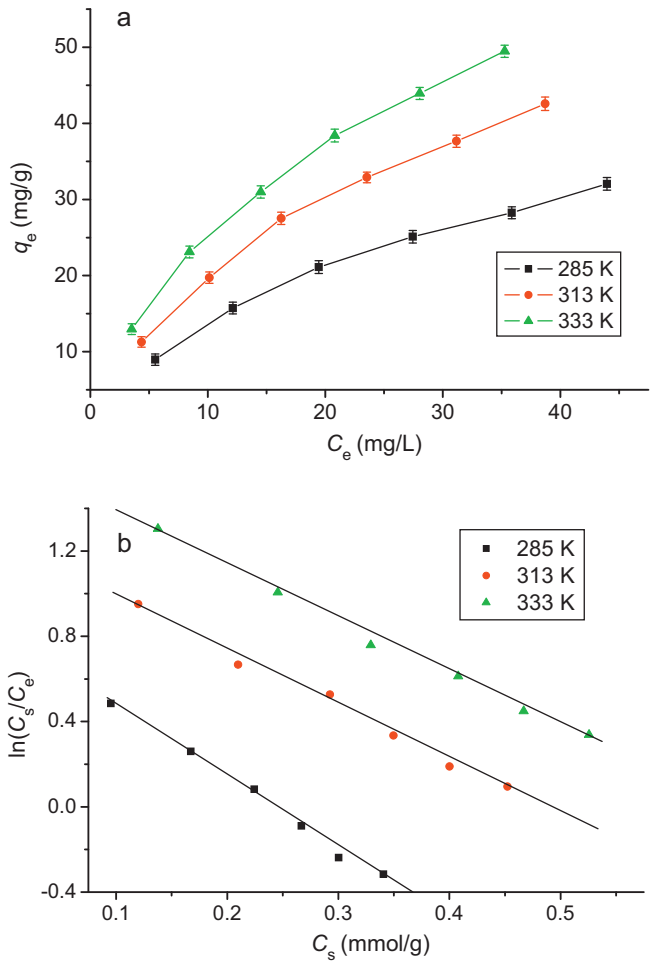

Fig. 7. (a) Temperature effect on phenol adsorbed by graphene, (b) plots of ln C_s/C_e versus C_s for calculation of thermodynamic parameters. The error bar represents the standard deviations (n = 3).

and shown in Fig. 7a. The results show that the equilibrium adsorption capacity of phenol increases with the increase in temperature from 285 to 333 K. Increasing adsorption capacities with increasing temperature indicates that the adsorption of phenol is controlled by an endothermic reaction.

In adsorption reaction thermodynamic parameters are used to judge whether the reaction occurs spontaneously or not. Thermodynamic parameters can be calculated from the variation of the thermodynamic equilibrium constant K_0 with the change in temperature [15]. For adsorption reactions, K_0 is defined as follows:

$$K_0 = \frac{a_s}{a_e} = \frac{\nu_s}{\nu_e}\frac{C_s}{C_e} \tag{8}$$

where a_s is the activity of adsorbed phenol, a_e is the activity of phenol in solution at equilibrium, C_s is the amount of phenol adsorbed by per mass of graphene (mmol/g), ν_s is the activity coefficient of the adsorbed phenol and ν_e is the activity coefficient of phenol in solution. As phenol concentration in the solution decreases and approaches zero, K_0 can be obtained by plotting ln(C_s/C_e) versus C_s and extrapolating C_s to zero (Fig. 7b) [15]. A linear regression analysis finds that the straight line fits the data well, the values of K_0 are obtained from the straight line intercept with the vertical axis. The calculated values of K_0 are 1.02, 1.24, and 1.62 at temperatures of 285, 313, and 333 K, respectively (Table 3).

Table 3
Thermodynamic parameters for phenol adsorbed by graphene.

Thermodynamic constant	Temperature (K)		
	285	313	333
K_0	1.03	1.24	1.62
ΔG° (cal/mol)	−48.80	−133.78	−319.21
ΔH° (cal/mol)	1817.40	1817.40	1817.40
ΔS° (cal/(mol K))	6.21	6.23	6.42

The average standard enthalpy change (ΔH°) is obtained from Van't Hoof equation:

$$\ln K_0(T_3) - \ln K_0(T_1) = \frac{-\Delta H^\circ}{R}\left(\frac{1}{T_3} - \frac{1}{T_1}\right) \tag{9}$$

where T_3 and T_1 are two different temperatures. The calculated value of ΔH° is 1064.54 cal/mol.

The adsorption standard free energy changes (ΔG°) can be calculated according to:

$$\Delta G^\circ = -RT\ln K_0 \tag{10}$$

where R is the universal gas constant (1.987 cal/(K mol)) and T is the temperature in Kelvin. The standard entropy change (ΔS°) can be obtained by:

$$\Delta S^\circ = -\frac{\Delta G^\circ - \Delta H^\circ}{T} \tag{11}$$

The thermodynamic parameters were listed in Table 3. The obtained values of ΔG° are −48.80, −133.78, and −319.21 cal/mol at temperatures of 285, 313, and 333 K, respectively. The negative values of ΔG° at three tested temperatures reveal that the adsorption is spontaneous process. It is reported [50] that a more negative ΔG° means a greater driving force of adsorption, resulting in a higher adsorption capacity. The higher negative value of ΔG° at 333 K than that at 285 K indicates that that adsorption is more spontaneous at high temperature. The positive values of ΔH° suggests that the interaction of phenol adsorbed by graphene is endothermic process, The positive values of ΔS° indicate increased randomness at the adsorbent/solution interface during the adsorption of phenol onto graphene [51].

4. Conclusions

Graphene was prepared using a modified Hummers' method. The BET characterization showed that the specific surface area, pore volume, and pore diameter of graphene were 305.78 m^2/g, 0.33 cm^3/g, and 3.63 nm, respectively. The solution pH played a significant role in influencing the adsorption capacity of graphene toward phenol molecules. The percent removal of phenol increased with the adsorbent dosage from 0.2 to 1.7 g/L and the adsorption capacity reached the maximum value of 28.26 mg/g at the dosage of 0.5 g/L. The pseudo second-order equation provided the better correlation for the adsorption data. The adsorption isotherm data were well fitted by both Freundlich and Langmuir models. Thermodynamic study showed that adsorption of phenol onto graphene was endothermic and spontaneous process.

Acknowledgements

This work was supported by the National Natural Science Foundation of China (50802045 and 20975056), SRF for ROCS, SEM, the Middle-aged and Youth Scientist Incentive Foundation of Shandong Province (BS09018) and the Taishan Scholar Program of Shandong Province, China.

References

[1] K.P. Singh, A. Malik, S. Sinha, P. Ojha, J. Hazard. Mater. 150 (2008) 626–641.
[2] A. Knop, L.A. Pilato, Phenolic Resins – Chemistry, Applications and Performance, Springer-Verlag, 1985.
[3] S. Sun, W. Wang, L. Zhang, M. Shang, J. Phys. Chem. C 113 (2009) 12826–12831.
[4] Y. Park, A.H.P. Skelland, L.J. Forney, J.H. Kim, Water Res. 40 (2006) 1763–1772.
[5] G. Moussavi, M. Mahmoudi, B. Barikbin, Water Res. 43 (2009) 1295–1302.
[6] Z. Wu, M. Zhou, Environ. Sci. Technol. 35 (2001) 2698–2703.
[7] R.S. Juang, W.C. Huang, Y.H. Hsu, J. Hazard. Mater. 164 (2009) 46–52.
[8] J.M. Li, X.G. Meng, C.W. Hu, J. Du, Bioresour. Technol. 100 (2009) 1168–1173.
[9] S. Froehner, R.F. Martinsa, W. Frukawa, M.R. Errera, Water Air Soil Pollut. 199 (2009) 107–113.
[10] N. Roostaei, F.H. Tezel, J. Environ. Manage. 70 (2004) 157–164.
[11] N. Calace, E. Nardi, B.M. Petronio, M. Pietroletti, Environ. Pollut. 118 (2002) 315–319.
[12] S. Kumar, M. Zafar, J.K. Prajapati, S. Kumar, S. Kannepalli, J. Hazard. Mater. 185 (2011) 287–294.
[13] E. Ballesteros, M. Gallego, M. Valcárcel, J. Chromatogr. A 869 (2000) 101–110.
[14] Y.H. Li, S.G. Wang, J.Q. Wei, X.F. Zhang, C. Cu, Z. Luan, D. Wu, B. Wei, Chem. Phys. Lett. 357 (2002) 263–266.
[15] Y.H. Li, Z. Di, J. Ding, D. Wu, Z. Luan, Y. Zhu, Water Res. 39 (2005) 605–609.
[16] S.V. Morozov, K.S. Novoselov, F. Shedin, D. Jiang, A.A. Firsov, A.K. Geim, Phys. Rev. B 72 (2005) 201401.
[17] A.A. Balandin, S. Ghosh, W.Z. Bao, I. Calizo, D. Teweldebrhan, F. Miao, C.N. Lau, Nano Lett. 8 (2008) 902–907.
[18] C.G. Lee, X.D. Wei, J.W. Kysar, J. Hone, Science 321 (2008) 385–388.
[19] S. Gilje, H. Song, M. Wang, K.L. Wang, R.B. Kaner, Nano Lett. 7 (2007) 3394–3398.
[20] P.K. Ang, W. Chen, A.T.S. Wee, K.P. Loh, J. Am. Chem. Soc. 130 (2008) 14392–14393.
[21] X. Liang, Z. Fu, S.Y. Chou, Nano Lett. 7 (2007) 3840–3844.
[22] X. Wang, L. Zhi, K. Mullen, Nano Lett. 8 (2008) 323–327.
[23] M.D. Stoller, S. Park, Y. Zhu, J. An, R.S. Ruoff, Nano Lett. 8 (10) (2008) 3498–3502.
[24] S. Stankovich, D.A. Dikin, G.H.B. Dommett, K.M. Kohlhaas, E.J. Zimney, E.A. Stach, R.D. Piner, S.T. Nguyen, R.S. Ruoff, Nature 442 (2006) 282–286.
[25] X. Deng, L. Lü, H. Li, F. Luo, J. Hazard. Mater. 183 (2010) 923–930.
[26] S.T. Yang, Y. Chang, H. Wang, G. Liu, S. Chen, Y. Wang, Y. Liu, A. Cao, J. Colloid Interface Sci. 351 (2010) 122–127.
[27] K. Zhang, V. Dwivedi, C. Chi, J. Wu, J. Hazard. Mater. 182 (2010) 162–168.
[28] T. Liu, Y.H. Li, Q. Du, J. Sun, Y. Jiao, G. Yang, Z. Wang, Y. Xia, W. Zhang, K. Wang, H. Zhu, D. Wu, Colloid Surf. B 90 (2012) 197–203.
[29] G. Zhao, L. Jiang, Y. He, J. Li, H. Dong, X. Wang, W. Hu, Adv. Mater. 23 (2011) 39593.
[30] G. Zhao, J. Li, X. Wang, Chem. Eng. J. 173 (2011) 185–190.
[31] C. Soldano, A. Mahmood, E. Dujardin, Carbon 48 (2010) 2127–2150.
[32] W.S. Hummers, R.E. Offeman, J. Am. Chem. Soc. 80 (1958) 1339.
[33] Y.H. Li, T. Liu, Q. Du, J. Sun, Y. Xia, Z. Wang, W. Zhang, K. Wang, H. Zhu, D. Wu, Mater. Res. Bull. Chem. Biochem. Eng. Q. 25 (2011) 483–491.
[34] M. Khalfaoui, S. Knani, M.A. Hachicha, A. Ben Lamine, J. Colloid Interface Sci. 263 (2003) 350–356.
[35] P.G. Ren, D.X. Yan, X. Ji, T. Chen, Z.M. Li, Nanotechnology 22 (2011) 055705.
[36] M. Tuzen, A. Sari, D. Mendil, O.D. Uluozlu, M. Soylak, M. Dogan, J. Hazard. Mater. 165 (2009) 566–572.
[37] J.F. Garcia-Araya, F.J. Beltran, P. Alvarez, F.J. Masa, Adsorption 9 (2003) 107–115.
[38] F.A. Banat, B. Al-Bashir, S. Al-Asheh, O. Hayajneh, Environ. Pollut. 107 (2000) 391–398.
[39] H.L. Wang, W.F. Jiang, Ind. Eng. Chem. Res. 46 (2007) 5405–5411.
[40] Y.S. Ho, G. McKay, Water Res. 34 (2000) 735–742.
[41] Y.S. Ho, G. McKay, Process Biochem. 34 (1999) 451–465.
[42] M. Sarkar, P.K. Acharya, B. Bhattacharya, J. Colloid Interface Sci. 266 (2003) 28–32.
[43] W.J. Weber, J.C. Morriss, J. Sanit. Eng. Div. Am. Soc. Civil Eng. 89 (1963) 31–60.
[44] W.H. Cheung, Y.S. Szeto, G. McKay, Bioresour. Technol. 98 (2007) 2897–2904.
[45] Ö. Gerçel, H.F. Gerçel, Chem. Eng. J. 132 (2007) 289–297.
[46] H.M.F. Freundlich, Z. Phys. Chem. 57 (1906) 385–471.
[47] I. Langmuir, J. Am. Chem. Soc. 38 (11) (1916) 2221–2295.
[48] W. Ma, F.Q. Ya, M. Han, R. Wang, J. Hazard. Mater. 143 (2007) 296–302.
[49] G.D. Sheng, D.D. Shao, X.M. Ren, X.Q. Wang, J.X. Li, Y.X. Chen, X.K. Wang, J. Hazard. Mater. 178 (2010) 505–516.
[50] K. Lin, J. Pana, Y. Chen, R. Cheng, X. Xu, J. Hazard. Mater. 161 (2009) 231–240.
[51] Y. Nuhoglu, E. Malkoc, Bioresour. Technol. 100 (2009) 2375–2380.